8-3-2020

Structure and Unprecedented Reactivity of a Mononuclear Nonheme Cobalt(III) Iodosylbenzene Complex

J. Yang

M. S. Seo

K. H. Kim

Y. M. Lee

S. Fukuzumi

See next page for additional authors

Repository Citation

Yang, J., Seo, M. S., Kim, K. H., Lee, Y. M., Fukuzumi, S., Shearer, J., & Nam, W. (2020). Structure and unprecedented reactivity of a mononuclear nonheme cobalt(III) iodosylbenzene complex. *Angewandte Chemie - International Edition, 59*(32), 13581-13585. https://doi.org/10.1002/anie.202005091

Authors

J. Yang, M. S. Seo, K. H. Kim, Y. M. Lee, S. Fukuzumi, Jason M. Shearer, and W. Nam

Amphoteric Reactivity | Hot Paper

How to cite: *Angew. Chem. Int. Ed.* **2020**, *59*, 13581–13585
International Edition: doi.org/10.1002/anie.202005091
German Edition: doi.org/10.1002/ange.202005091

Structure and Unprecedented Reactivity of a Mononuclear Nonheme Cobalt(III) Iodosylbenzene Complex

Jindou Yang[+], Mi Sook Seo[+], Kyung Ha Kim, Yong-Min Lee, Shunichi Fukuzumi, Jason Shearer,* and Wonwoo Nam**

Abstract: *A mononuclear nonheme cobalt(III) iodosylbenzene complex, $[Co^{III}(TQA)(OIPh)(OH)]^{2+}$ (**1**), is synthesized and characterized structurally and spectroscopically. While **1** is a sluggish oxidant in oxidation reactions, it becomes a competent oxidant in oxygen atom transfer reactions, such as olefin epoxidation, in the presence of a small amount of proton. More interestingly, **1** shows a nucleophilic reactivity in aldehyde deformylation reaction, demonstrating that **1** has an amphoteric reactivity. Another interesting observation is that **1** can be used as an oxygen atom donor in the generation of high-valent metal-oxo complexes. To our knowledge, we present the first crystal structure of a Co^{III} iodosylbenzene complex and the unprecedented reactivity of metal-iodosylarene adduct.*

High-valent metal-oxo species and their precursors, such as metal-hydroperoxo, -peroxo, and -superoxo complexes, have been synthesized, characterized spectroscopically and/or structurally, and investigated in reactivity studies as the chemical models of biologically important metal-oxygen intermediates in the dioxygen activation and oxidation reactions by metalloenzymes.[1–4] Regarding reactivities of the metal–oxygen intermediates, metal-oxo complexes are electrophilic oxidants in biological and abiological oxidation reactions,[2–4] whereas metal-peroxo complexes are nucleophiles that effect the deformylation of aldehydes.[5,6] Recently, it has been demonstrated that metal-hydroperoxo complexes are active oxidants in both electrophilic and nucleophilic reactions with an amphoteric character.[7] In the case of metal-superoxo complexes, the electrophilic character of the metal-superoxo intermediates has been well demonstrated in biological and abiological oxidation reactions.[8,9]

Iodosylarenes (ArIO), including iodosylbenzene (PhIO), are versatile oxidants frequently used in the catalytic oxidation of organic substrates as well as in the generation of metal-oxo intermediates.[10] Metal-iodosylarene adducts have been considered as potent oxidants in oxidation reactions as well as the precursors of metal-oxo species,[11] and some of the metal-ArIO adducts have been structurally characterized recently.[12] Their electrophilic reactivities have also been demonstrated in oxygen atom transfer (OAT) and C–H activation reactions.[11,12] Very recently, Anderson and coworkers reported the crystal structures of Co^{II}-iodosylarene and Co^{II}-iodosylarene adducts.[13] However, to our knowledge, there is no report on the structure and chemical reactivity of Co^{III}-iodosylbenzene species. Herein, we report for the first time the synthesis and structural and spectroscopic characterization of a Co^{III}-iodosylbenzene complex, $[Co^{III}(TQA)(OIPh)(OH)]^{2+}$ (**1**, TQA = tris(2-quinolylmethyl)amine; Scheme 1). We also report the reactivity of **1** in OAT, C–H activation, and aldehyde deformylation reactions in the presence of a small amount of acid (Scheme 1). The use of **1** as a terminal oxidant in the synthesis of high-valent metal-oxo complexes is also demonstrated (Scheme 1).

The starting cobalt complex, $[Co^{II}(TQA)(CF_3SO_3)(CH_3CN)]^+$ (**2**), was synthesized and structurally and spectroscopically characterized (see Supporting Information: Experimental Section, Tables S1 and S2, and Figures S1 and S2). When **2** was treated with 5 equivalents of PhIO in

[*] J. Yang,[+] Dr. M. S. Seo,[+] K. H. Kim, Dr. Y.-M. Lee, Prof. Dr. S. Fukuzumi, Prof. Dr. W. Nam
Department of Chemistry and Nano Science
Ewha Womans University
Seoul 03760 (Korea)
E-mail: fukuzumi@chem.eng.osaka-u.ac.jp
wwnam@ewha.ac.kr

Prof. Dr. J. Shearer
Department of Chemistry
Trinity University
San Antonio, TX 78212 (USA)
E-mail: jshearer@trinity.edu

Prof. Dr. W. Nam
School of Chemistry and Chemical Engineering, Shaanxi Normal University
Xi'an 710119 (China)

[+] These authors contributed equally to this work.

Supporting information and the ORCID identification number(s) for the author(s) of this article can be found under: https://doi.org/10.1002/anie.202005091.

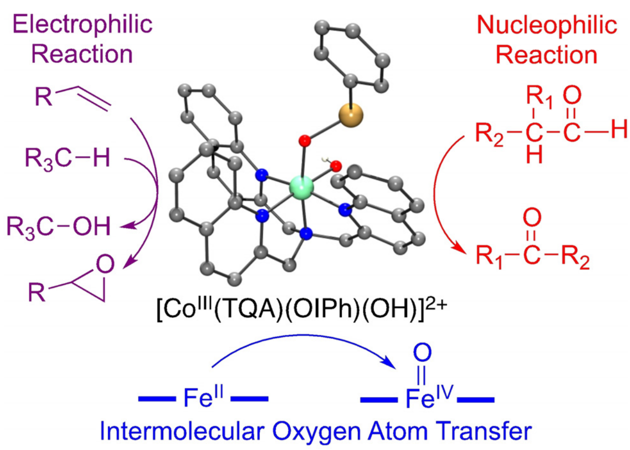

Scheme 1. $[Co^{III}(TQA)(OH)(OIPh)]^{2+}$ (**1**) and its reactivities in olefin epoxidation, C–H activation, aldehyde deformylation, and intermolecular OAT reactions in the presence of HOTf. Co light blue, O red, I gold, N dark blue, C gray.

CH_3CN at −40 °C, an immediate UV/Vis spectral change was observed (blue spectrum in Figure 1 a), followed by the relatively slow formation of a green species (red spectrum in Figure 1 a), denoted as **1**. It is likely that the fast UV/Vis spectral change in the first step is due to the formation of a Co^{III}(OH) species, as proposed in the reaction of a Mn^{III} complex and PhIO,[12e] and the second step is an exchange of a *cis*-binding ligand (e.g., an anionic ligand, $CF_3SO_3^-$) with PhIO to generate **1**. Complex **1** is highly stable in CH_3CN at −40 °C (Figure S3a), allowing us to characterize it spectroscopically and crystallize it for X-ray crystal structure.

Compound **1** exhibited an electronic absorption band at 645 nm ($\varepsilon = 220\,M^{-1}cm^{-1}$) with a shoulder at 550 nm ($\varepsilon = 200\,M^{-1}cm^{-1}$; Figure 1 a). The X-band electron paramagnetic resonance (EPR) spectrum of **1** is silent, indicating that **1** contains a diamagnetic Co^{3+} ion (Figure S3b); this is supported by Evans' nuclear magnetic resonance (NMR) method measurement demonstrating that **1** is indeed diamagnetic ($S = 0$) (see Supporting Information: Experimental Section). The cold-spray ionization time-of-flight mass (CSI-MS) spectrum of **1** showed mass peaks at m/z 368.1 and 885.1 corresponding to $[Co^{III}(TQA)(OIPh)(OH)]^{2+}$ and $[Co^{III}(TQA)(OIPh)(OH)(OTf)]^+$ (**1**-^{16}O), respectively (Figure 1 b; also see Figure S4). When **1** was generated with PhI^{18}O, mass peaks corresponding to $[Co^{III}(TQA)(^{18}OIPh)(OH)]^{2+}$ and $[Co^{III}(TQA)(^{18}OIPh)(^{16}OH)(OTf)]^{2+}$ (**1**-^{18}O) appeared at m/z 369.1 and 887.1, respectively (Figure 1 b, right panel in inset; also see Figure S4). Further, upon addition of $H_2{}^{18}O$ to **1**-^{18}O, the mass peaks at m/z 369.1 and 887.1 further shifted to 370.1 and 889.1 corresponding to $[Co^{III}(TQA)(^{18}OIPh)(^{18}OH)]^{2+}$ and $[Co^{III}(TQA)(^{18}OIPh)(^{18}OH)(OTf)]^+$, respectively (Figure S4), resulting from the exchange of the hydroxide ligand ($^{16}OH^-$) with $H_2{}^{18}O$. The resonance Raman (rRaman) spectrum of **1**, recorded upon 405 nm excitation in a frozen CH_3CN:CF_3CH_2OH (v:v = 3:1) solution, displayed an isotopically sensitive band at 671 cm^{-1}, which shifted to 634 cm^{-1} upon ^{18}O-substitution (Figure 1 c). The observed isotope shift of −37 cm^{-1} is in good agreement with the calculated value for a diatomic I−O bond oscillator (−34 cm^{-1}). The band at 671 cm^{-1} is comparable to the I–O stretching bands of metal-iodosylbenzene complexes.[11a,d,12c,e] A week isotope sensitive band at 496 cm^{-1}, which was shifted to 484 cm^{-1} upon ^{18}O substitution, was assigned as a Co-OIPh stretching vibration.[7b,14]

Co K-edge X-ray absorption spectroscopic studies were undertaken on frozen CH_3CN solutions of **1** and **2** (Figure 2; Table S3). A blue-shift in the edge position of **1** (7720.8(2) eV) versus **2** (7119.3(2) eV) was observed, consistent with a Co^{III} oxidation state for **1**. Weak pre-edge features corresponding to nominal Co(1s→3d) transitions were observed for **2** (7709.1(1) eV) and **1** (7710.4(1) eV), consistent with six-

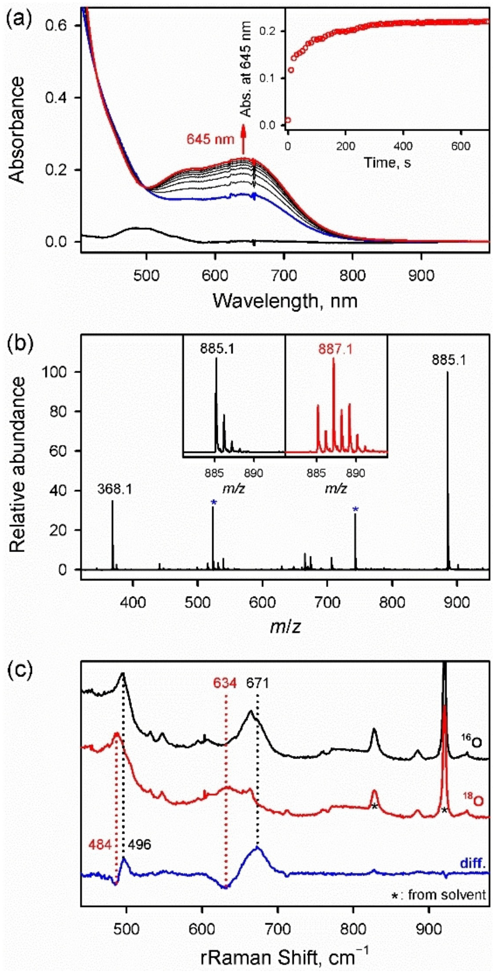

Figure 1. a) UV/Vis spectral changes in the reaction of **2** (1.0 mM, black) with PhIO (5.0 mM) in CH_3CN at −40 °C. b) CSI-MS spectrum of **1**. The peaks at m/z 368.1 and 885.1 correspond to **1**-^{16}O. Peaks with an asterisk are from polymeric iodosylbenzene. Insets show observed isotope distribution patterns for **1**-^{16}O (red) and **1**-^{18}O (black). c) rRaman spectra of **1**-^{16}O (black line) and **1**-^{18}O (red line) upon excitation at 405 nm in frozen CH_3CN. Blue line shows the difference spectrum of **1**-^{16}O and **1**-^{18}O.

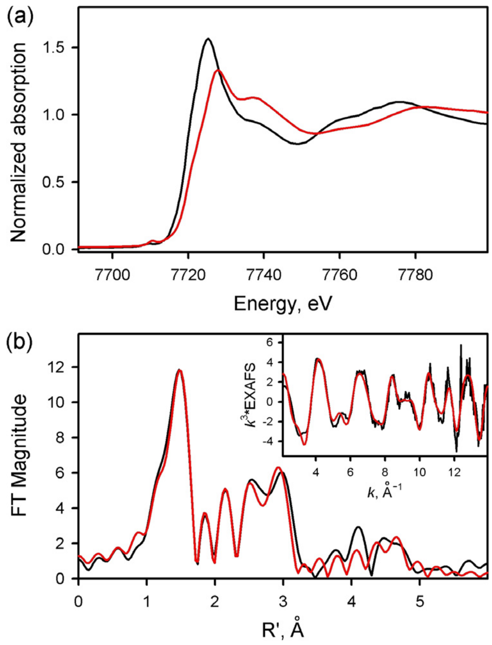

Figure 2. a) Co K-edge XANES of **1** (red) and **2** (black). b) Magnitude FT k^3 EXAFS and k^3 EXAFS (inset) of **1**. The black spectra depict the experimental data and the red spectra depict the best fit to the data.

coordinate cobalt centers for both **1** and **2**. The extended X-ray absorption fine structure (EXAFS) region of **1** was modeled as six-coordinate cobalt with two short Co–O bonds (1.87 Å) and four Co–N bonds (2.00 Å). Pathways for an outer sphere Co⋯I interaction (3.66 Å) and a Co-O-I multiple scattering pathway were also required to model the EXAFS data. Taken together, these data indicate that six-coordinate **1** possesses a PhIO and an O(H) ligand to Co^{III} (see below).

Crystals suitable for X-ray diffraction (XRD) were obtained by diffusing diethyl ether slowly into a CH_3CN solution of **1** at −40 °C (See Supporting Information for CCDC numbers and Tables S1 and S2 for crystallographic data of **1**). The ORTEP structure of **1** reveals a mononuclear end-on cobalt(III)-iodosylbenzene complex in a distorted octahedral geometry (Figure 3). The Co–OIPh bond length is 1.8997(2) Å, which is longer than the Co–OH distance (1.8759(2) Å). The O–I bond (1.9307(1) Å) is comparable to those of other metal-iodosylbenzene adducts, such as $[Mn^{III}(L)(OIPh)(OH)]^{2+}$ (1.929(5) Å)[12e] and $[Fe^{III}(L)(OIPh)]^{2+}$ (1.920(3) Å),[12b] but slightly shorter than that of $Mn^{IV}(L)(OIAr)_2$ (1.954 and 1.984 Å)[12a] and slightly longer than that of $[Co^{II}(L)(OIPh)]^+$ (1.878(6) Å).[13]

We then investigated the reactivity of **1** in OAT reactions. Upon the addition of PPh_3 to a solution of **1** at −40 °C, the absorption band at 645 nm corresponding to **1** disappeared within approximately 500 s (Figure S5); the organic product, $O{=}PPh_3$ (93 % yield) and the Co^{III} product were analyzed spectroscopically (Figure S6). Further reactivity studies of **1** were performed with olefins. First, addition of styrene to **1** resulted in no spectral change even at 25 °C (Figure S7a). Interestingly, addition of 1.2 equivalents of triflic acid (HOTf) to the solution of **1** containing styrene at 25 °C resulted in the decrease of the absorption band at 645 nm due to **1**, accompanied by the increase of the absorption band at 550 nm due to $[Co^{III}(TQA)(OH)]^{2+}$ (Figures S7b and S8). The organic product(s) was also analyzed by ^{1}H NMR spectroscopy and GC-MS, showing the formation of phenylacetaldehyde (92 % yield) (Figures S9–S11). In kinetic study, the reaction of **1** and styrene obeyed the first-order kinetics under the pseudo-first-order conditions (Figure S7b), yielding a second-order rate constant (k_2) of $1.9\times10^{-2}\,M^{-1}s^{-1}$ at 25 °C (Figure S7c). Similarly, k_2 values of *para*-substituted styrene derivatives were determined (Table S4 and Figure S12). A plot of the logarithm of the k_2 values versus the one-electron oxidation potentials of substrates afforded a slope of −5.1 (Figure S13), indicating the electrophilic character of **1**.

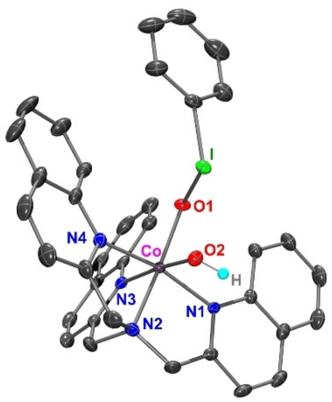

Figure 3. ORTEP diagram of **1** with thermal ellipsoids set at 50 % probability. Hydrogen atoms are omitted for clarity except for the hydroxo hydrogen atom (C gray; H cyan; N blue; O red; I green; Co violet).

The reactivity of **1** was also investigated in the C–H bond activation reactions with the C–H bond dissociation energy (BDE) values of hydrocarbons in the range of 75.5–81 kcal mol^{-1}, such as triphenylmethane (TPM, 81 kcal mol^{-1}), fluorine (80 kcal mol^{-1}), 1,4-cyclohexadiene (CHD, 78 kcal mol^{-1}), 9,10-dihydroanthracene (DHA, 77 kcal mol^{-1}), and xanthene (75.5 kcal mol^{-1}).[15] Addition of DHA to a solution of **1** resulted in the disappearance of the intermediate with a first-order decay profile, and a second-order rate constant of $4.9\times10^{-2}\,M^{-1}s^{-1}$ at 25 °C with the kinetic isotope effect (KIE) value of 2.2(3) was determined in the hydroxylation of DHA-h_4/d_4 (Figure S14). Product analysis for the reaction solution of **1** and DHA revealed the formation of anthracene (95 % yield) as a sole organic product and $[Co^{III}(TQA)(OH)]^{2+}$ as the cobalt-containing decay product of **1** (Figure S15). In addition, the second-order rate constants with other substrates, such as xanthene, CHD, fluorene, and, TPM, were also determined (Table S5 and Figure S16), showing the decrease of the k_2 values with the increase of the BDEs of substrates C–H bonds (Figure S17). These results suggest that a hydrogen atom abstraction from the substrates C–H bond by **1** is the rate-determining step, as frequently observed in metal-oxo chemistry.[2,3] It should be noted that the reactivity of **1** in HAT reactions did not change in the presence of excess PhI, indicating that **1** is the active oxidant.

Interestingly, **1** is capable of participating in aldehyde deformylation reactions. Upon the addition of 2-phenylpropionaldehyde (2-PPA) to **1** under an Ar atmosphere, **1** decayed with a first-order kinetics profile, and a second-order rate constant, k_2(H), of $4.2\times10^{-2}\,M^{-1}s^{-1}$ at 25 °C was obtained (Figure S18). **1** reacted with deuterated α-[D]-2-PPA under the identical conditions, and a second-order rate constant, k_2(D), was determined to be $5.8\times10^{-2}\,M^{-1}s^{-1}$ at 25 °C, giving an inverse KIE ratio of 0.72 (Figure S18b). Product analysis of the reaction solution revealed the formation of acetophenone as a deformylated product (98 % yield), as frequently observed in the nucleophilic oxidative reactions by metal-peroxo and -hydroperoxo complexes.[5–7]

We also employed **1** as a terminal oxidant to generate high-valent metal-oxo species (Scheme 2, reaction *b*), as PhIO has been frequently used as an artificial oxidant in such reactions (Scheme 2, reaction *a*).[2c,e,3a,e,10] Addition of $[Fe(TMC)]^{2+}$ (TMC = 1,4,8,11-tetramethyl-1,4,8,11-tetraazacyclotetradecane) to **1** at 25 °C afforded UV/Vis absorption spectral changes with isosbestic points at 600 and 700 nm, in which the absorption band at 645 nm due to **1** decreased with the increase of the characteristic absorption band of $[Fe^{IV}(O)(TMC)]^{2+}$ at 820 nm (Figure 4; also see Figure S19).[16] To our knowledge, the present study reports the first example of using a metal-iodosylbenzene adduct as a terminal oxidant for the generation of high-valent metal-oxo species.

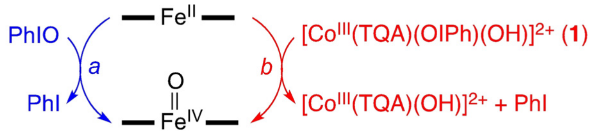

Scheme 2. PhIO (reaction *a*) and Co^{III}-OIPh (reaction *b*) in the generation of iron(IV)-oxo species from iron(II) complex.

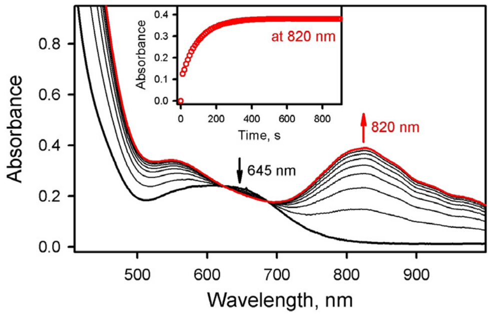

Figure 4. UV/Vis spectral changes for the formation of $[Fe^{IV}(O)(TMC)]^{2+}$ (red line) in the reaction of **1** (1.0 mм, black line) and $[Fe^{II}(TMC)]^{2+}$ (1.0 mм) in the presence of HOTf (1.2 mм) in CH_3CN at 25 °C. Inset: the time trace monitored at 820 nm for the formation of $[Fe^{IV}(O)(TMC)]^{2+}$.

In conclusion, we have reported for the first time the X-ray crystal structure of a mononuclear nonheme Co^{III}-OIPh adduct, $[Co^{III}(TQA)(OIPh)(OH)]^{2+}$, which exhibits an amphoteric reactivity in electrophilic and nucleophilic reactions in the presence of a small amount of proton. We have also shown that metal iodosylarene complexes can be used as a terminal oxidant for the generation of metal-oxo species. In future studies, we will focus on elucidating the detailed mechanisms of metal-iodosylarene species in oxidation reactions as well as in the OAT reaction for the formation of metal-oxo species. We are currently investigating the effects of protons and metal ions on the reactivity of metal-iodosylarene species.[17]

Acknowledgements

This work was supported by the NRF of Korea through CRI (NRF-2012R1A3A2048842 to W.N.), Basic Science Research Program (2017R1D1A1B03029982 to Y.-M.L., 2017R1D1A1B03032615 to S.F., and 2019R1I1A1A01055822 to M.S.S.) and the NSF of USA (CHE-1900380 and CHE-1854854 to J.S.). X-ray absorption data were collected on beamline 07ID-2 at the Canadian Light Source, which is supported by the CFI, NSERC, NRC, CIHR, the Government of Saskatchewan, and the University of Saskatchewan.

Conflict of interest

The authors declare no conflict of interest.

Keywords: aldehyde deformylation reaction · amphoteric reactivity · cobalt(III) complexes · iodosylbenzene adducts · nonheme complexes

[1] a) W. Nam, *Acc. Chem. Res.* **2007**, *40*, 465, and references therein; b) L. Que, *J. Biol. Inorg. Chem.* **2017**, *22*, 171, and references therein.

[2] a) M. Guo, T. Corona, K. Ray, W. Nam, *ACS Cent. Sci.* **2019**, *5*, 13; b) K. D. Dubey, S. Shaik, *Acc. Chem. Res.* **2019**, *52*, 389; c) X. Huang, J. T. Groves, *Chem. Rev.* **2018**, *118*, 2491; d) R. A. Baglia, J. P. T. Zaragoza, D. P. Goldberg, *Chem. Rev.* **2017**, *117*, 13320; e) W. Nam, *Acc. Chem. Res.* **2015**, *48*, 2415.

[3] a) W. Nam, Y.-M. Lee, S. Fukuzumi, *Acc. Chem. Res.* **2014**, *47*, 1146; b) S. A. Cook, A. S. Borovik, *Acc. Chem. Res.* **2015**, *48*, 2407; c) M. Puri, L. Que, Jr., *Acc. Chem. Res.* **2015**, *48*, 2443; d) S. Hong, Y.-M. Lee, K. Ray, W. Nam, *Coord. Chem. Rev.* **2017**, *334*, 25; e) J. J. D. Sacramento, D. P. Goldberg, *Acc. Chem. Res.* **2018**, *51*, 2641; f) Y. Liu, T.-C. Lau, *J. Am. Chem. Soc.* **2019**, *141*, 3755; g) V. Larson, B. Battistella, K. Ray, N. Lehnert, W. Nam, *Nat. Rev. Chem.* **2020**, doi.org/10.1038/s41570-020-0197-9.

[4] a) R. Trammell, K. Rajabimoghadam, I. Garcia-Bosch, *Chem. Rev.* **2019**, *119*, 2954; b) S. M. Adam, G. B. Wijeratne, P. J. Rogler, D. E. Diaz, D. A. Quist, J. J. Liu, K. D. Karlin, *Chem. Rev.* **2018**, *118*, 10840; c) C. E. Elwell, N. L. Gagnon, B. D. Neisen, D. Dhar, A. D. Spaeth, G. M. Yee, W. B. Tolman, *Chem. Rev.* **2017**, *117*, 2059; d) D. A. Quist, D. E. Diaz, J. J. Liu, K. D. Karlin, *J. Biol. Inorg. Chem.* **2017**, *22*, 253.

[5] J. Cho, R. Sarangi, W. Nam, *Acc. Chem. Res.* **2012**, *45*, 1321.

[6] a) P. Barman, P. Upadhyay, A. S. Faponle, J. Kumar, S. S. Nag, D. Kumar, C. V. Sastri, S. P. de Visser, *Angew. Chem. Int. Ed.* **2016**, *55*, 11091; *Angew. Chem.* **2016**, *128*, 11257; b) P. Barman, F. G. C. Reinhard, U. K. Bagha, D. Kumar, C. V. Sastri, S. P. de Visser, *Angew. Chem. Int. Ed.* **2019**, *58*, 10639; *Angew. Chem.* **2019**, *131*, 10749.

[7] a) M. Sankaralingam, Y.-M. Lee, W. Nam, S. Fukuzumi, *Coord. Chem. Rev.* **2018**, *365*, 41; b) B. Kim, D. Jeong, T. Ohta, J. Cho, *Commun. Chem.* **2019**, *2*, 81; c) S. H. Bae, X.-X. Li, M. S. Seo, Y.-M. Lee, S. Fukuzumi, W. Nam, *J. Am. Chem. Soc.* **2019**, *141*, 7675; d) M. Sankaralingam, Y.-M. Lee, S. H. Jeon, M. S. Seo, K.-B. Cho, W. Nam, *Chem. Commun.* **2018**, *54*, 1209; e) J. Cho, S. Jeon, S. A. Wilson, L. V. Liu, E. A. Kang, J. J. Braymer, M. H. Lim, B. Hedman, K. O. Hodgson, J. S. Valentine, E. I. Solomon, W. Nam, *Nature* **2011**, *478*, 502.

[8] a) J. M. Bollinger, Jr., C. Krebs, *Curr. Opin. Chem. Biol.* **2007**, *11*, 151; b) S. Fukuzumi, Y.-M. Lee, W. Nam, *Dalton Trans.* **2019**, *48*, 9469; c) H. Noh, J. Cho, *Coord. Chem. Rev.* **2019**, *382*, 126.

[9] a) W. D. Bailey, N. L. Gagnon, C. E. Elwell, A. C. Cramblitt, C. J. Bouchey, W. B. Tolman, *Inorg. Chem.* **2019**, *58*, 4706; b) A. R. Corcos, O. Villanueva, R. C. Walroth, S. K. Sharma, J. Bacsa, K. M. Lancaster, C. E. MacBeth, J. F. Berry, *J. Am. Chem. Soc.* **2016**, *138*, 1796; c) S. Hong, K. D. Sutherlin, J. Park, E. Kwon, M. A. Siegler, E. I. Solomon, W. Nam, *Nat. Commun.* **2014**, *5*, 5440; d) P. Pirovano, A. M. Magherusan, C. McGlynn, A. Ure, A. Lynes, A. R. McDonald, *Angew. Chem. Int. Ed.* **2014**, *53*, 5946; *Angew. Chem.* **2014**, *126*, 6056.

[10] a) V. V. Zhdankin, J. D. Protasiewicz, *Coord. Chem. Rev.* **2014**, *275*, 54; b) A. Yoshimura, V. V. Zhdankin, *Chem. Rev.* **2016**, *116*, 3328.

[11] a) M. Guo, Y.-M. Lee, M. S. Seo, Y.-J. Kwon, X.-X. Li, T. Ohta, W.-S. Kim, R. Sarangi, S. Fukuzumi, W. Nam, *Inorg. Chem.* **2018**, *57*, 10232; b) Y. Kang, X.-X. Li, K.-B. Cho, W. Sun, C. Xia, W. Nam, Y. Wang, *J. Am. Chem. Soc.* **2017**, *139*, 7444; c) B. Wang, Y.-M. Lee, M. S. Seo, W. Nam, *Angew. Chem. Int. Ed.* **2015**, *54*, 11740; *Angew. Chem.* **2015**, *127*, 11906; d) S. Hong, B. Wang, M. S. Seo, Y.-M. Lee, M. J. Kim, H. R. Kim, T. Ogura, R. Garcia-Serres, M. Clémancey, J.-M. Latour, W. Nam, *Angew. Chem. Int.*

Ed. **2014**, *53*, 6388; *Angew. Chem.* **2014**, *126*, 6506; e) P. Leeladee, D. P. Goldberg, *Inorg. Chem.* **2010**, *49*, 3083; f) S. H. Wang, B. S. Mandimutsira, R. Todd, B. Ramdhanie, J. P. Fox, D. P. Goldberg, *J. Am. Chem. Soc.* **2004**, *126*, 18; g) K. P. Bryliakov, E. P. Talsi, *Angew. Chem. Int. Ed.* **2004**, *43*, 5228; *Angew. Chem.* **2004**, *116*, 5340; h) W. Nam, Y. O. Ryu, W. J. Song, *J. Biol. Inorg. Chem.* **2004**, *9*, 654; i) J. A. Smegal, C. L. Hill, *J. Am. Chem. Soc.* **1983**, *105*, 2920.

[12] a) C. Wang, T. Kurahashi, H. Fujii, *Angew. Chem. Int. Ed.* **2012**, *51*, 7809; *Angew. Chem.* **2012**, *124*, 7929; b) A. Lennartson, C. J. McKenzie, *Angew. Chem. Int. Ed.* **2012**, *51*, 6767; *Angew. Chem.* **2012**, *124*, 6871; c) C. Wang, T. Kurahashi, K. Inomata, M. Hada, H. Fujii, *Inorg. Chem.* **2013**, *52*, 9557; d) C. Wegeberg, C. G. Frankær, C. J. McKenzie, *Dalton Trans.* **2016**, *45*, 17714; e) D. Jeong, T. Ohta, J. Cho, *J. Am. Chem. Soc.* **2018**, *140*, 16037.

[13] E. A. Hill, M. L. Kelty, A. S. Filatov, J. S. Anderson, *Chem. Sci.* **2018**, *9*, 4493.

[14] S. Kim, C. Saracini, M. A. Siegler, N. Drichko, K. D. Karlin, *Inorg. Chem.* **2012**, *51*, 12603.

[15] Y.-R. Luo, *Handbook of Bond Dissociation Energies in Organic Compounds*, CRC, New York, **2002**.

[16] J.-U. Rohde, J.-H. In, M. H. Lim, W. W. Brennessel, M. R. Bukowski, A. Stubna, E. Münck, W. Nam, L. Que, Jr., *Science* **2003**, *299*, 1037.

[17] The effects of Lewis and Brønsted acids on the reactivities of metal-oxygen intermediates have been highlighted recently: a) S. Bang, Y.-M. Lee, S. Hong, K.-B. Cho, Y. Nishida, M. S. Seo, R. Sarangi, S. Fukuzumi, W. Nam, *Nat. Chem.* **2014**, *6*, 934; b) S. Fukuzumi, K. Ohkubo, Y.-M. Lee, W. Nam, *Chem. Eur. J.* **2015**, *21*, 17548; c) J. Chen, H. Yoon, Y.-M. Lee, M. S. Seo, R. Sarangi, S. Fukuzumi, W. Nam, *Chem. Sci.* **2015**, *6*, 3624; d) S. Hong, Y.-M. Lee, M. Sankaralingam, A. K. Vardhaman, Y. J. Park, K.-B. Cho, T. Ogura, R. Sarangi, S. Fukuzumi, W. Nam, *J. Am. Chem. Soc.* **2016**, *138*, 8523; e) S. H. Bae, Y.-M. Lee, S. Fukuzumi, W. Nam, *Angew. Chem. Int. Ed.* **2017**, *56*, 801; *Angew. Chem.* **2017**, *129*, 819; f) T. Devi, Y.-M. Lee, W. Nam, S. Fukuzumi, *J. Am. Chem. Soc.* **2018**, *140*, 8372.

Manuscript received: April 8, 2020
Accepted manuscript online: May 2, 2020
Version of record online: May 26, 2020